JOURNAL OF SOLID STATE CHEMISTRY **127,** 92–97 (1996)
ARTICLE NO. 0361

Molecular Dynamics Simulation of the Structure of Calcium Silicate Hydrates

I. $Ca_{4+x}Si_6O_{14+2x}(OH)_{4-2x}(H_2O)_2$ $(0 \leq x \leq 1)$

P. Faucon,*[,1] J. M. Delaye,† and J. Virlet‡

Service de Physique de l'Etat Condensé, †Section de Recherche de Metallurgie Physique, and ‡Service de Chimie Moléculaire, C.E.A. Saclay, 91191 Gif sur Yvette, France

Received February 9, 1996; in revised form August 9, 1996; accepted August 14, 1996

Molecular dynamics has been used to simulate the structure of calcium silicate hydrates (CSH) having Ca/Si ratios of 0.66 and 0.83. In the absence of labile calcium, silicon nuclear magnetic resonance (NMR) shows that the tetrahedral chains move closer together than predicted by the tobermorite model initially adopted. This proximity may lead to bridging between the chains. In the presence of labile calcium, there is a partial rupture of the chains, as seen with NMR. The instability of the bridging tetrahedra in the initial structure causes this rupture. The dissociation of a water molecule releases the oxygen necessary for the reaction. The rupture of the chains creates two new types of tetrahedra in the structure (Q1(2H) and Q1(1H)). © 1996 Academic Press, Inc.

INTRODUCTION

Calcium silicate hydrates (CSH) are the main components of cements. They are characterized by an X-ray diffraction pattern with few peaks (1). Without being amorphous, they therefore have a structure organized over distances of less than 100 Å. X-ray diffraction has not resolved their structure, but has demonstrated structural similarities with tobermorite. These similarities have also been established by ^{29}Si magic-angle-spinning nuclear magnetic resonance spectroscopy (MAS-NMR) (2–4).

CSH have a variable stoichiometry (5) and are commonly defined by their Ca/Si ratio. In this study, we focused solely on CSH(I) of Ca/Si ratios 0.66 and 0.83 whose structures are the closest to that of 11 Å tobermorite (6). The composition of tobermorite is $Ca_{4+x}Si_6O_{14+2x}(OH)_{4-2x}$ $(H_2O)_2$, generally with $0.66 \leq x \leq 0.83$. There is "Dreierketten" in tobermorite, whose structure is derived from that of wollastonite and has been studied by X-ray diffraction (8, 9) and by electron diffraction. This structure is monoclinic, space group $P2_1$, with lattice constants of $a_m = 6.69$ Å, $b_m = 7.39$ Å, $c_m = 22.779$ Å, and $\gamma = 123.49$. It is, however, easier to work in the pseudo orthorhombic cell ($a_o = 11.16$ Å, $b_o = 7.39$ Å, $c_o = 22.779$ Å) which yields the representation shown in Fig. 1. Tobermorite has infinite chains of silicon tetrahedra which run between layers of calcium atoms. One calcium layer in three is "labile"; i.e., the calcium atoms are statistically distributed among the sites. At a Ca/Si ratio of 0.66, the labile layers are empty. As the Ca/Si ratio increases, the labile layer is progressively occupied. The maximum occupancy observed in natural tobermorites is seen for Ca/Si = 0.83: sites Ca(5) and Ca(6) are 50% occupied. For Ca/Si = 0.66, the oxygens O(8), O(9), O(14), and O(18) of the bridging tetrahedra (Si(3) and Si(5)) are hydroxylated. The incorporation of labile calcium atoms in the structure creates an excess positive charge, which is compensated by the loss of the protons of these oxygens. The number of water molecules intercalated between the chains of tetrahedra and the labile calcium layers is constant over the 0.66 < Ca/Si < 0.83 range. The H_2O/Si ratio is 0.33.

X-ray diffraction spectra indicate that CSH(I) of molar ratio 0.66 < Ca/Si < 0.83 have a structure similar to that of tobermorite, which was therefore used as a structural model (6).

Silicon-29 MAS-NMR revealed that to a first approximation the CSH(I) are characterized by two contributions. The first is always observed between -85 and -86 ppm with respect to tetramethylsilane (TMS), and is similar to that seen with 14 Å tobermorite (2). This Q2-type signal indicates that each silicon tetrahedron is linked to two other silicon tetrahedra. When the Ca/Si ratio increases from 0.66 to 0.83, a second signal characteristic of Q1 (silicon tetrahedra linked to a single tetrahedron) appears around 79 ppm (2, 3). Silicon NMR thus shows that as the Ca/Si molar ratio in the CSH(I) is increased, breaks occur in the chains of tetrahedra, which are of infinite length in tobermorite.

NMR provides information on the environment of the

---

[1] To whom correspondence should be addressed.

0022-4596/96 $18.00

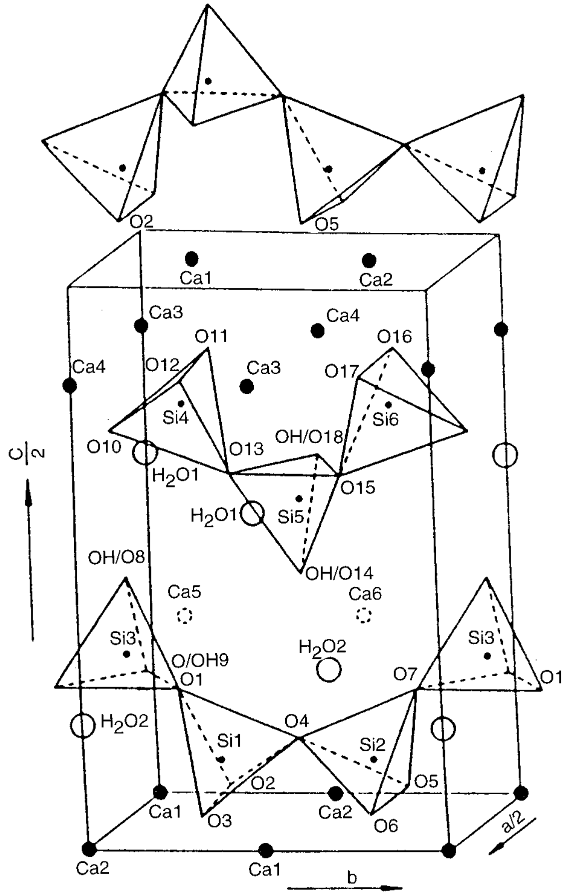

FIG. 1. The 11 Å tobermorite structure using the orthorhombic cell ($a/2$ = 5.58 Å, b = 7.39 Å, $c/2$ = 11.389 Å). Ca(5) and Ca(6) are statistically distributed (9).

silicon, but does not give the full structure. Molecular dynamics simulation gives atomic-level information which complements NMR data. We studied the relaxation of the tobermorite structure in order to identify the sources of structural instability and to understand the mechanisms causing breaks in the chains. First, we established the conditions of stability of 11 Å tobermorite (Ca/Si = 0.66), whose structure is similar to that of CHS of the same Ca/Si ratio. Under these conditions, we introduced calcium into the CSH structure to reveal the mechanisms whereby rupture occurs in the chains of tetrahedrally coordinated silicon, as the Ca/Si ratio increases.

COMPUTATIONAL PROCEDURE

The interatomic potentials used in the molecular dynamics simulations comprise two- and three-body potentials. The Born–Mayer–Huggins types of potentials were used to model the Si–O, Si–Si, Si–Ca, Si–H, O–O, O–Ca, O–H, and Ca–Ca interactions. For a pair of atoms i–j separated by a distance r_{ij}, the potential energy attributed to this pair is given by the following expression:

$$\phi(r_{ij}) = A_{ij} \exp\left(-\frac{r_{ij}}{\rho_{ij}}\right) + \frac{q_i q_j}{4\pi\varepsilon 0 r_{ij}} \operatorname{erfc}\left(\frac{r_{ij}}{\alpha}\right).$$

The values of the parameters A_{ij} and ρ_{ij} are given in Table 1. We chose to truncate the Coulombic interaction by means of the "erfc" function. The parameter α regulates the range of this interaction. This approximation reduces calculation time but introduces an error. Neglecting the long-range Coulombic interactions is equivalent to discounting the effect of the mean electric field produced by long-range order. We shall see that this does not prevent us from stabilizing the structure of tobermorite.

The relative stabilities of each site are essentially related to their local order, and the hierarchy of site stability is not perturbed by neglecting the long-range Coulombic interactions. Feuston *et al.* chose values of about 0.2 Å for α (10), which is too low to stabilize the tobermorite. We assigned a value of 7 Å. The atomic charges used for the Coulombic interactions are formal (Si^{4+}, O^{2-}, Ca^{2+}, H^{+}).

To improve the representation of local order, three-body terms were applied to the angles O–Si–O, Si–O–Si, Si–O–H and H–O–H. These terms have the following form:

$$\phi_3(r_{ij}, r_{ik}, \phi_{jik}) = \lambda_i \exp\left(\frac{\gamma_i}{r_{ij} - r_{ci}} + \frac{\gamma_i}{r_{ik} - r_{ci}}\right)$$
$$(\cos\theta_{jik} - \cos\theta_0)^2$$

r_{ij} and r_{ik} represent, respectively, the distances between the atoms i and j, and i and k, of the triplet (j, i, k). θ_{jik} is

TABLE 1
Parameters for Two-Body Potentials (10, 11)

	A_{ij} (10^{-9} erg)	ρ_{ij} (Å)
Si–Si	1.877	0.29
Si–O	2.962	0.29
Si–H	0.069	0.29
O–O	0.725	0.29
O–H	0.3984	0.29
H–H	0.034	0.35
Si–Ca	7.2	0.29
O–Ca	10.5104	0.29
Ca–Ca	27,373	0.29

TABLE 2
Parameters for Three-Body Potentials (10)

	λ (10^{-11} erg)	γ(Å)	r_o(Å)	θ_0
O–Si–O	19.0	$\gamma_{Si-O} = 2.8$	3.0	109.5°
Si–O–Si	0.3	$\gamma_{O-Si} = 2.0$	2.6	109.5°
Si–O–H	5.0	$\gamma_{O-Si} = 2.0$ $\gamma_{O-H} = 1.2$	$r_{O-Si} = 2.6$ $r_{O-H} = 1.5$	109.5°
H–O–H	35.0	1.3	1.6	104.5°

TABLE 4
Protons and Labile Calcium Atoms Introduced into the Unit Cell for Ca/Si Ratios of 0.66 and 0.83

Ca/Si	Protonated oxygens	Labile Ca
0.66	O(8), O(9), O(14), O(18) H_2O(1) and H_2O(2)	—
0.83	O(8), O(14) H_2O(1) and H_2O(2)	Ca(5): one in two sites Ca(6): one in two sites

the angle ⟨j-i-k⟩. The values of the adjustable parameters are given in Table 2.

To represent the H_2O molecules, and their possible dissociation into one H^+ and one OH^-, additional pair potentials were introduced for the Si–H, H–H and O–H interactions. These terms have the following form (10, 13):

$$\phi(r_{ij}) = \frac{a_{ij}}{1 + \exp(b_{ij}/(r_{ij} - c_{ij}))}.$$

A single additional term was applied to the Si–H interactions; two were applied to the H–H interactions, and three to the O–H interactions. The values of the parameters are given in Table 3. The atomic positions in the initial cell are those proposed by Hamid for 11 Å tobermorite. The hydrogens were placed randomly at about 1 Å from the hydroxylated oxygens OH and H_2O. For the structure with a Ca/Si molar ratio of 0.83, calcium atoms were introduced into the labile layer (Table 4). We verified that the results did not depend on the initial positions of the labile calciums.

The parallelepiped simulation cell contains a entire number of orthorhombic cells of tobermorite, and is repeated to infinity by periodic conditions.

The presence of hydrogen atoms (mass 18 times less than that of oxygen) imposes 10^{-16} s time steps for the molecular dynamics simulation. To minimize computation time, the preliminary calculations were done for cells of about 600 atoms, depending on the Ca/Si ratio, thus reproducing the initial cell four times. We then validated the results on cells of more than 2000 atoms, reproducing the initial cell 16-fold.

TABLE 3
Parameters for Additional Water Potentials (10, 13)

	a_{ij}(10^{-11}erg)	b_{ij}(Å)	c_{ij}(Å)
Si–H	−4.6542	6.0	2.2
H–H	−5.2793	6.0	1.51
	0.3473	2.0	2.42
O–H	−2.0840	15.0	1.05
	7.6412	3.2	1.50
	−0.8336	5.0	2.0

The calculations were performed with a constant-volume algorithm, and the successive positions of the atoms were determined by the classical equations of Verlet. The use of formal charges necesitated adjustment of the cell volume. If this adjustment is not made, the electrostatic interactions, in particular with the hydrogens, are too strong and destabilize the structure. The unit cell was therefore expanded by 10% along each axis (yielding a density of 1.8 g/cm^3) in order to stabilize Hamid's structure.

Before each simulation, a 1500-step quenching sequence moved each ion along the lines of force acting on it to the nearest equilibrium site. This technique allowed initial adjustment of the position of the H^+ ions in the H_2O molecules.

The cells containing four unit cells are relaxed at between 100 and 450 K; those with 16 unit cells are relaxed between 300 and 800 K.

RESULTS

A preliminary study of the coordination of silicon, and of the Si–O distances in the relaxed structures, showed that silicon was always tetrahedrally coordinated, with a mean Si–O distance of 1.6 Å. The mean O–H distances were always 1 Å. The distributions for the H–O–H and Si–O–H angles were centered on respective values of 104.5° and 109.5°. Three-body potentials therefore allowed reproduction of local angular order, when the binding was strongly covalent.

CSH with a Ca/Si Ratio of 0.66

The relaxation at 800 K of a cell of 2432 atoms, like that of a cell of 608 atoms at 300 K, induced no break in the network of tetrahedrally coordinated silicons. The final cell, in fact, contained solely Q2-type tetrahedra (tetrahedra linked to two other tetrahedra). The structure therefore comprised tetrahedral chains of infinite length. This is to be expected since the cell volume was adjusted so as to stabilize Hamid's structure.

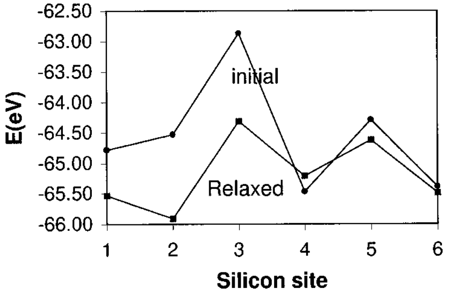

FIG. 2. Potential energies for silicons before and after relaxation for a Ca/Si ratio of 0.66 (cell of 2368 atoms, density 1.8 g/cm^3, relaxed at 800 K).

The energy of an atomic site was calculated by assigning half of each pair potential to each of the two constituent atoms. For three-body potentials, the energy was entirely assigned to the central site, and was low compared with the pair potentials. Figure 2 shows that in the initial structure, the silicon atoms with the least cohesive energy were the bridging tetrahedra (Si(3) and Si(5) in Fig. 1). The main effect of relaxation was to lower the energy of the Si(3) site, which remained the most unstable site after molecular dynamics simulation.

The Si(3)–Si(5) distance decreased from 0.509 to 0.42 nm after relaxation. The absence of labile calcium energetically favored the drawing together of the tetrahedral chains, which was also enhanced when the density increased. Figure 3 illustrates the change in the Si(3)–Si(5) distance as a function of cell density. In a 608-atom cell at 300 K, the higher the cell density, the greater the post-relaxation reduction in the mean Si(3)–Si(5) distance. When the Si(3)–Si(5) distances were similar to the Si(1)–Si(3) distances, there was bridging between the chains and the formation of Q3 tetrahedra (tetrahedra linked to three other tetrahedra). ^{29}Si-MAS-NMR spectra recorded in cross polarization reveal the presence of Q3 tetrahedra in the structure of CSH of low Ca/Si ratio (3, 4). This may be due to the instability of the Si(3) and Si(5) sites.

The OH groups, and the H_2O molecules, were preserved by the molecular dynamics simulation. The energies of the sites occupied by oxygen atoms (Table 5) show that the oxygens of the water molecules were less stable than the other oxygens.

TABLE 5

Potential Energies of the Different Sites Occupied by Oxygens for a Ca/Si Ratio of 0.66 (Cell of 2,432 Atoms, Density 1.8 g/cm^3, Relaxed at 800 K)

	Si–O–Si	Si–O–Ca	Si–O–H	H–O–H
E initial (eV)	−19.29	−15.74	−16.67	−13.98
E final (eV)	−18.87	−15.82	−16.30	−15.14

CSH with a Ca/Si Ratio of 0.83

The temperature-dependent relaxation of the 592-atom cells revealed the instability of the initial structure (Fig. 4). Below 200 K, the relaxation of the cell yielded a structure similar to the initial structure, which was metastable up to 200 K. Above 200 K, the relaxation led to a structure of much lower cohesive energy which was stable above 200 K. The energy required to leave the metastable state corresponds to a thermal agitation of 200 K. Figure 5 shows that the structural transformation occurring around 200 K promoted the formation of Q1 tetrahedra. There was therefore a break in the tetrahedrally coordinated silicon chains. The relaxed structure contains a mean of about 16% Q1 tetrahedra.

The kinetics of formation of the relaxed structure of the 2,368-atom cell (Fig. 6) were much slower than those of the 592-atom cell. Equilibrium was reached in 10 ps only when the relaxation occurred at 800 K, whereas 200 K was enough for the 592-atom cell. At a given temperature, the 2368-atom cell remained stable longer, because the deformations of the chains of SiO_4 tetrahedra had less effect on the overall structure. Periodic conditions resulted in a high density of deformations in the small simulation cell, whose stability was increasingly affected. The final structure of a cell of 2368 atoms contained about 15% Q1

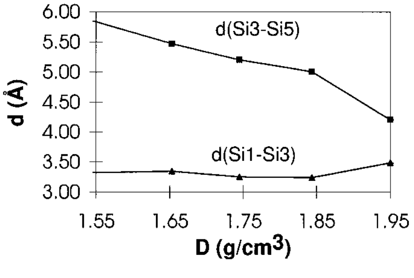

FIG. 3. Change in interchain distance as a function of density for a Ca/Si ratio of 0.66 (cell of 608 atoms, relaxed at 300 K).

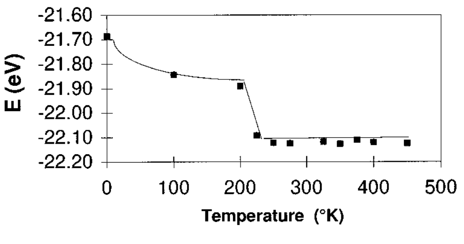

FIG. 4. Mean potential energy per atom as a function of temperature for a Ca/Si ratio of 0.83 (cell of 592 atoms, density 1.8 g/cm^3).

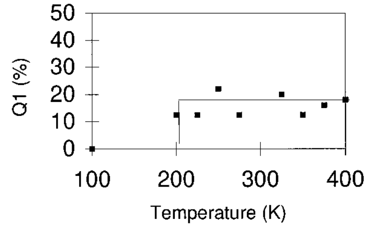

FIG. 5. Demonstration of chain rupture for a Ca/Si ratio of 0.83 (cell of 592 atoms, density 1.8 g/cm^3).

tetrahedra. The 592- and 2368-atom cells therefore had similar structures.

Despite the incorporation of calcium into the labile layer of the initial structure, the Si(3) site, and to a lesser degree the Si(5) site, remained less stable than the other sites (Fig. 7). The rupture of the chains of tetrahedra occurred around these more fragile sites, between Si(3) and Si(1) (Fig. 8), and stabilized them energetically. Despite the break, all the silicons were tetrahedrally coordinated. This was possible because the water molecule $H_2O(2)$ dissociated, thereby providing Si(3) with the oxygen needed to preserve its tetrahedral coordination.

DISCUSSION

Molecular dynamics simulation of structures revealed two types of relaxation mechanism.

Bridging between Chains

The instability of the Si(3) and Si(5) sites seems to cause the changes in the initial structure. When the Ca/Si molar ratio is 0.66, this instability causes the chains to move closer together: the Si(3)–Si(5) distance decreases. If the density of the cell is increased slightly (Fig. 3), this distance is shortened enough for Q3 tetrahedra to form, through bridging between the two chains and formation of a water molecule:

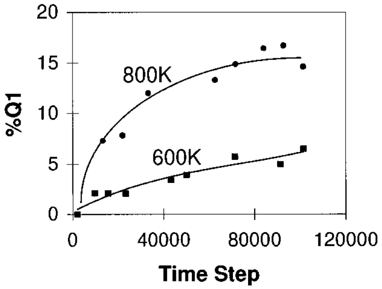

FIG. 6. Kinetics of formation of the relaxed structure for a cell of 2368 atoms of Ca/Si ratio 0.83 (density 1.8 g/cm^3).

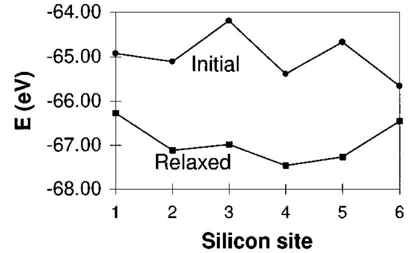

FIG. 7. Potential energies for silicons before and after relaxation for a Ca/Si ratio of 0.83 (cell of 2368 atoms, density 1.8 g/cm^3, relaxed at 800 K).

$$\text{Si(3)–O(8)H} + \text{Si(5)–O(14)H} \rightarrow \text{Si(3)–O–Si(5)} + H_2O.$$

The above reaction is also observed at a Ca/Si molar ratio of 0.83, since Q3 tetrahedra are present in the relaxed structure, albeit in low proportion (2 to 3%). In fact, the introduction of labile calcium atoms limits the convergence of the chains. For a relaxed structure of density 1.8 g/cm^3 at 800 K, the mean distance between two bridging tetrahedra lengthens from 0.42 to 0.46 nm when the Ca/Si ratio increases from 0.66 to 0.83.

Rupture of the Chains

The incorporation of labile calcium atoms into the network leads principally to the rupture of some of the chains of tetrahedra. At a relaxation temperature of 800 K, and a density of 1.8 g/cm^3, CSH with a Ca/Si ratio of 0.66 contains 100% Q2 tetrahedra. At a Ca/Si ratio of 0.83, the instability of the Si(3) site (Fig. 7) results in rupture of some of the chains (Fig. 8). The rupture involves the tetrahedra of sites Si(3) and Si(5), via dissociation of the $H_2O(2)$ molecule. The two hydrogens provided by the water explain why the two nonbridging oxygens created by the

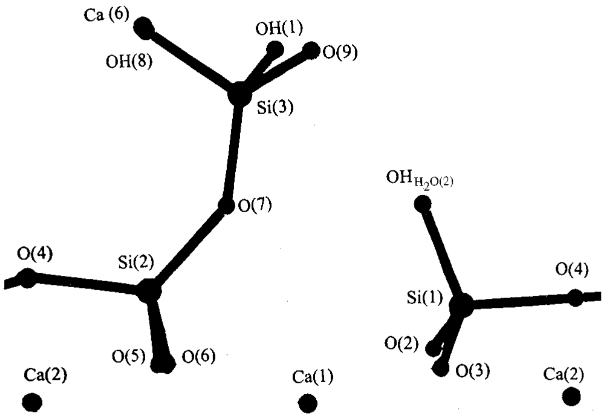

FIG. 8. Q1 tetrahedra in the relaxed structure with a Ca/Si ratio of 0.83 (cell of 2368 atoms, density 1.8 g/cm^3, relaxed at 800 K).

TABLE 6

Types of Tetrahedrally Coordinated Silicon Present for a Ca/Si Ratio of 0.83 (Cell of 2,368 Atoms, Density 1.8 g/cm^3, Relaxed at 800 K)

Q1(Si(1))	Q1(Si(2))	Bridging Q2	Nonbridging Q2	Q3
8%	8%	24%	58%	2%

dissociation are hydroxylated. The mechanism is therefore as follows:

$$\mathrm{Si(3)\text{–}O(1)\text{–}Si(1)} + \mathrm{H_2O} \rightarrow \mathrm{Si(3)\text{–}O(1)H} + \mathrm{Si(1)\text{–}OH}.$$

The structure contains 33% Si(3) and Si(1) tetrahedra, and about 15% Q1 tetrahedra are formed, so at least one Si(3) in two is dissociated. Q1 (Si(3)) tetrahedra alternate with the Q2 (Si(3)) tetrahedra. This dissociation leads to the formation of two types of Q1 tetrahedra. Before relaxation, the Si(3) tetrahedron possesses a single hydroxyl, O(8)H, whereas the Si(1) tetrahedron has none. After relaxation, two types of Q1 tetrahedra form: the Q1 (Si(3)) tetrahedra with two OH, and the Q1 (Si(1)) tetrahedra with just one. The Qn percentages are indicated in Table 6.

CONCLUSIONS

Molecular dynamics simulation aids understanding of certain silicon NMR data concerning CSH with $0.66 < \mathrm{Ca/Si} < 0.83$. The structure of tobermorite has long served as a model for this type of CSH. We observed a lower proportion of Q1 tetrahedra than Q3 tetrahedra, as also seen by NMR. In the absence of labile calcium atoms, the chains of tetrahedra converge, thereby reducing the instability of the Si(3) site. No break in the chains is observed. The introduction of labile calcium atoms into the structure results in the formation of Q1 tetrahedra. The break occurs between the Si(3) and Si(1) tetrahedra, via a water molecule, which dissociates, thereby enabling four-coordination to be preserved for each tetrahedron. The hydrogens released by the dissociation allow the formation of two new OH bonds with the two Q1 tetrahedra. As Si(3) already has an OH group, two types of Q1 tetrahedra are created by rupture of the chains (Si(3) → Q1(2H), Si(1) → Q1(1H)).

ACKNOWLEDGMENTS

We express particular thanks to M. Nonat, of the Laboratoire de Réactivité des Solides at the Université de Dijon, and M. Jacquinot, of the NMR laboratory of the CEA (Commissariat à l'Energie Atomique), for helpful discussions about the structure of the CSH. We are also grateful to the Agence Nationale pour les Dechets Radioactifs (ANDRA) for cofinancing this study with the CEA.

REFERENCES

1. H. F. W. Taylor, *J. Chem. Soc.* **33,** 163 (1953).
2. M. Grutzeck, A. Benesi, and B. Fanning, *J. Am. Ceram. Soc.* **72**(4), 665 (1989).
3. Y. Okada, H. Ishida, and T. Mitsuda, *J. Am. Ceram. Soc.* **77**(3), 765 (1994).
4. X. Cong and R. J. Kirckpatrick, *Adv. Chem. Res.* **27**(7), 103 (1995).
5. S. A. Greenberg and T. N. Chang, *J. Phys. Chem.* **69,**1151 (1965).
6. H. F. W. Taylor, *J. Am. Ceram. Soc.* **69**(6), 464 (1986).
7. J. C. C. McConnell, *Mineral. Mag.* **30,** 293 (1954).
8. H. D. Megaw and C. H. Kelsey, *Nature* **177,** 390 (1956).
9. S. A. Hamid, *Z. Kristallogr.* **154,** 189 (1981).
10. B. P. Feuston and S. H. Garofalini, *J. Phys. Chem.* **94,** 5351 (1990).
11. T. F. Soules, *J. Chem. Phys.* **71**(11), 4570 (1979).
12. M. M. Probst, T. Radnai, K. Heinzinger, P. Bopp, and B. M. Rode, *J. Phys. Chem.* **89,** 753 (1985).
13. F. H. Stillinger and A. Rahman, *J. Chem. Phys.* **68**(2), 666 (1978).